*Supporting Information for*

# Bioinspired Fabrication of DNA-Inorganic Hybrid Composites Using Synthetic DNA

Eunjung Kim,[1] Shweta Agarwal,[1] Nayoung Kim,[1] Fredrik Sydow Hage,[2] Vincent Leonardo,[1] Amy Gelmi,[1] and Molly M. Stevens[1]*

[1]Department of Materials, Department of Bioengineering and Institute for Biomedical Engineering, Imperial College London, London, SW7 2AZ, United Kingdom

[2]SuperSTEM Laboratory, SciTech Daresbury Campus, Daresbury WA4 4AD, United Kingdom

Correspondence to:

*Email: m.stevens@imperial.ac.uk

## EXPERIMENTAL SECTION

**Agarose and Polyacrylamide Gel Electrophoresis.** The DNA samples were analyzed by 0.8% megabase agarose gel (Bio-Rad, USA) electrophoresis in 1× Tris/borate/EDTA (TBE) buffer. The gel was run at 50 V for 10 min and 100 V for 30 min, stained with SYBR Gold stain (Thermo Fisher Scientific) for 30 min at room temperature, and visualized with the BioSpectrum Imaging System (Ultra-Violet Products, UK). 2.5 kb DNA marker (Bio-Rad) and 1.0 kbp DNA marker (Thermo Fisher Scientific) were used as the reference standard. The gel images were processed with ImageJ software.

For native polyacrylamide gel electrophoresis, the prepared samples were run on a 10% polyacrylamide gel in 1× TBE buffer at 50 V for 10 min and 100 V for 60 min. For denaturing polyacrylamide gel electrophoresis, the samples were resolved on a 10% polyacrylamide gel containing 7 M urea in 1× TBE buffer at 80 V for 10 min and 120 V for 60 min. The urea-polyacrylamide gels were warmed by pre-running at 200 V for 1 h prior to loading and washed with 1× TBE buffer to remove excess urea. The samples were loaded after denaturation at 90 °C for 5 min in TBE-urea sample loading buffer. The gels were stained with SYBR Gold for 30 min and imaged with the BioSpectrum Imaging System. 10 bp DNA marker (Thermo Fisher Scientific) was used as the reference standard, and the obtained images were processed with ImageJ software.

**AFM Imaging and Indentation Study.** For sample preparation, the AmpDNA or λ DNA (1 μg $mL^{-1}$) was diluted in 10 mM HEPES buffer (pH 7.5) containing 5 mM nickel chloride, deposited onto a freshly cleaved mica sheet, and left to stand at room temperature for 10 min. The mica sheet was then rinsed with nuclease-free water several times to remove salts and unbound DNA

and dried with compressed air. Atomic force microscopy (AFM) imaging was conducted on an AFM 5500 microscope (Agilent Technologies, USA) in tapping mode in air. A HQ:NSC15/Al BS tip (MikroMasch, Germany) was used for the topography imaging. The images were processed with Gwyddion software.

To determine the Young's modulus of $Mg_2PPi$/DNA composites ($Mg_2PPi$, $Mg_2PPi$/AmpDNA, $Mg_2PPi$/λ DNA, and DNF), indentation experiments were conducted on an AFM 5500 microscope using the HQ:NSC15/Al BS cantilever with a calibrated spring constant of 5 N $m^{-1}$. Five particles per sample were indented with between one to five measurements per particle. The obtained force-distance curves were fitted using the free software AtomicJ.[1] The Young's modulus was calculated using the Hertz model assuming spherical indentation. The model was limited to an indentation depth less than 10% of the particle height in order to avoid substrate stiffness influence. Data are presented as mean Young's modulus ± standard error.

**Analysis of the Nature of AmpDNA as RCA Products.** To probe the nature of RCA products, comprehensive analysis of AmpDNA was performed using several enzymes and SYBR dyes specific for single-stranded (ssDNA) and/or double-stranded DNA (dsDNA) cleavage and staining. For enzyme digestion, two purified RCA products were prepared by performing RCA reaction at 30 °C for 20 h in the absence and presence of PPase (2 mU $\mu L^{-1}$), indicative of DNA strands present in DNF particles and AmpDNA strands (referred to as AmpDNA(-PPase) and AmpDNA(+PPase), respectively). For efficient isolation of DNA, $Mg_2PPi$ precipitates in RCA products were dissolved by adding 20 mM EDTA solution at a 1:1 volume ratio and purified by ethanol precipitation. After purification, the resulting DNA was thermally fragmented by heating at 95 °C for 15 min to reduce the viscosity of highly concentrated intact AmpDNA, facilitating

easy control of DNA over the reaction with enzymes. The AmpDNA(-PPase) and AmpDNA(+PPase) were digested with four nucleases, including exonuclease I (Exo I), exonuclease III (Exo III), and exonuclease VII (Exo VII) obtained from New England Biolabs, and duplex-specific nuclease (DSN, Evrogen) at the optimized conditions. As a control, phage λ DNA, M13mp18 ssDNA (New England Biolabs), and synthetic 50 nt ssDNA oligonucleotide (Integrated DNA Technology, see the sequences in Table S1) were also tested. All DNA samples (45 μg $mL^{-1}$, 15 μL) were incubated in a reaction volume of 20 μL containing enzymes (20 U of Exo I, 100 U of Exo III, 10 U of Exo VII, and 0.25 U of DSN) at 37 °C (with Exo I, III, and VII) or 60 °C (with DSN) for 2 h. The reaction buffers provided from suppliers were used without modification. The digested products were resolved by 0.8% megabase agarose gel and 10% native polyacrylamide gel electrophoresis in 1× TBE buffer with post-staining using SYBR Gold stain.

The serial 2-fold dilutions of the purified AmpDNA(-PPase) and AmpDNA(+PPase) (initial concentration: 1 μg $mL^{-1}$) were further stained with 2× SYBR Green I, SYBR Green II, and SYBR Gold (Thermo Fisher Scientific) in parallel in TE buffer (10 mM Tris-HCl, 1 mM EDTA, pH 8.0). The mixtures were then incubated in a 96-well plate at room temperature for 15 min. The same concentrations of λ DNA and M13mp18 ssDNA were used as a control. The fluorescence intensity of SYBR Green I and SYBR Green II was recorded at an excitation of 497 nm and an emission of 520 nm using the EnVision multilabel plate reader. The fluorescence intensity of SYBR Gold was recorded at an excitation of 495 nm and an emission of 537 nm.

**EcoRV Restriction Enzyme Treatments.** In this experiment, different template DNA minicircles were used by replacing six base sequences of linear template with the restriction site

GATATC recognized by EcoRV restriction endonuclease (New England Biolabs) (See Table S1 for details of nucleic acid sequences). To obtain AmpDNA, the RCA was performed with newly synthesized template DNA minicircles in the absence or presence of PPase in a final volume of 50 μL, and the RCA products were subsequently purified with ethanol and salt precipitation as described in Materials and Methods. The isolated AmpDNA was eluted in 100 μL of 10 mM Tris buffer (pH 8.0), and DNA concentration and purity were determined by PicoGreen assay and NanoDrop. The average repeating units in AmpDNA were estimated by following the procedures reported by Y. Li *et al.*[2,3] In detail, prior to digestion the AmpDNA (0.5 μL, 25 ng $\mu L^{-1}$) was hybridized with primers (1 μL, 100 μM) by heating at 90 °C for 5 min and slowly cooling to room temperature over 3 h. The resulting AmpDNA (0.6 ng $\mu L^{-1}$) was digested by EcoRV (5 U $\mu L^{-1}$) in 20 μL of CutSmart buffer (New England Biolabs) at 37 °C for 2 h. 2 μL of digestion products was then mixed with 1 μL of 50 nt DNA oligonucleotide (100 μM) as a loading control and 3 μL of 2× TBE-urea loading buffer, and analyzed by 10% denaturing urea-polyacrylamide gel electrophoresis.

**SIM Imaging.** For super-resolution structured illumination microscopy (SIM) imaging, a protein was chemically labeled with a primary amine-reactive fluorescent dye. Briefly, RNase A (2.5 mg $mL^{-1}$) was reacted with 5/6-carboxyfluorescein succinimidyl ester (fluorescein-NHS) at a 1:15 molar ratio in 50 mM borate buffer (pH 9.0) at room temperature for 4 h. Excess dyes were removed from the dye-labeled RNase A using a centrifugal filter device (MWCO 10 kDa) and redispersed in 50 mM Tris buffer (pH 8.0). The protein concentration was determined using a NanoDrop 2000c spectrometer (Thermo Fisher Scientific). The AmpDNA was enzymatically labeled with a dye through direct incorporation of Cyanine 3-deoxyuridine triphosphate (Cy3-

dUTP) to the growing DNA strands during RCA reaction. Fluorescent AmpDNA was obtained by performing RCA in the presence of Cy3-dUTP (0.2 mM) and PPase (2 mU $\mu L^{-1}$) at 30 °C for 20 h, followed by purification with ethanol precipitation. The $Mg_2PPi$-R and $Mg_2PPi$/AmpDNA with fluorescently modified AmpDNA (26.7 μg $mL^{-1}$) and RNase A (200 μg $mL^{-1}$) were prepared using the co-precipitation method. The DNF and DNF-R were also fabricated by adding fluorescent RNase A (600 μg $mL^{-1}$) and Cy3-dUTP (0.2 mM) to the RCA reaction solution. The growth of those particles and purification by centrifugation were carried out in the same procedures as described above. 10 μL of the particles in nuclease-free water was briefly mixed into 190 μL of VectaShield mounting media (Vector Laboratories) and was pipetted onto an APTES-treated ibidi 8-well glass bottom μ-slide. The particles were left overnight to allow them to settle to the base of the slide. SIM imaging was then performed with the Zeiss Elyra PS1 system (Carl Zeiss, Germany).

**Table S1.** Nucleic acid sequences used in this study.

| Name | Sequence (5' – 3') |
|---|---|
| Linear template DNA | Phosphorylation-AAT ATT ATT CCA GCT GGC GCT CGA GCT CGA GCC AGG TTG TAT CGT GAG ACT GCA CCT TGA ACG CTT ATT ATG ATT |
| Linear template DNA for EcoRV digestion | Phosphorylation -AAT ATT ATT CCA GCT GGC GCT CGA G***GA TAT C***CC AGG TTG TAT CGT GAG ACT GCA CCT TGA ACG CTT ATT ATG ATT |
| Primer for RCA | AAT AAT ATT AAT CAT AAT A |
| Primer for EcoRV digestion | GCT CGA G***GA TAT C***CC AGG TT |
| DNA as a loading control | ATT CCA GCT AAA CTC CCT GTA TCA AGC GTT TTC GGC AAA CCT GCT TCA TC |

Letters in bold indicate the recognition site for EcoRV enzyme. Underlined sequences 'CTCGAG' in linear template DNA were replaced with the sequences 'GATATC' for EcoRV digestion.

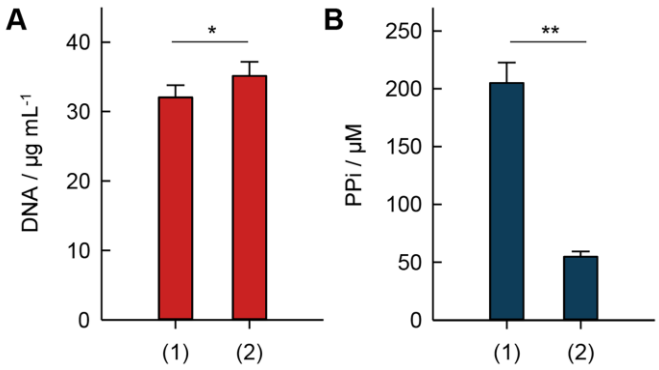


**Figure S1.** Quantification of (A) DNA and (B) PPi concentrations of AmpDNA isolated from the RCA reaction in the (1) absence and (2) presence of PPase. Data represent mean ± s.d. for N = 5. *$p < 0.05$ and **$p < 0.001$ determined by two-tailed *t*-test.

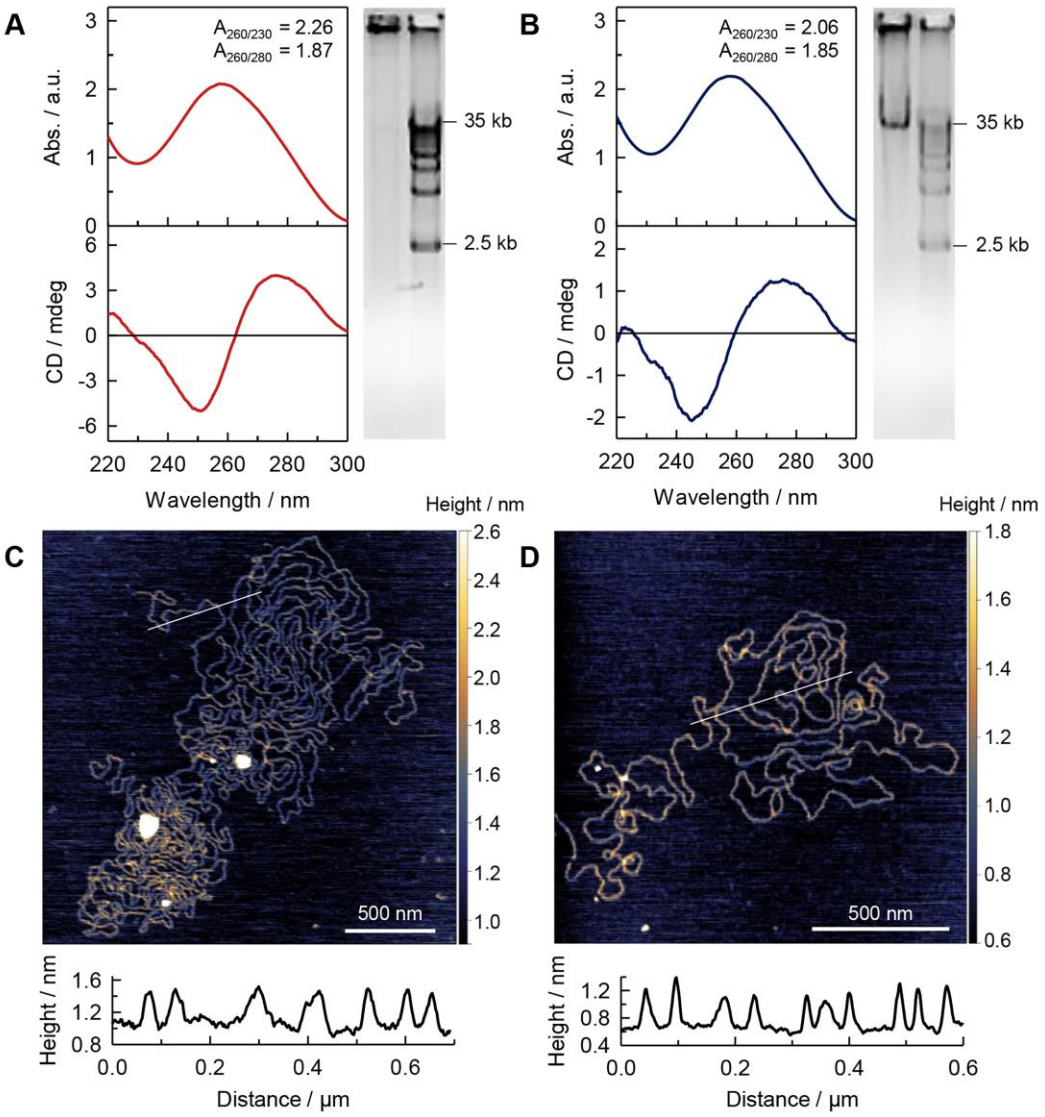


**Figure S2.** Characterization of AmpDNA and comparison with λ DNA. UV absorption and CD spectra of (A) AmpDNA and (B) λ DNA. Both DNA were resolved on a 0.8% megabase agarose gel. 2.5 kb DNA marker was used as a reference. Representative AFM images of (C) AmpDNA and (D) λ DNA with corresponding height profiles of the DNA products marked in (C) and (D). The measured height was 0.47 ± 0.03 nm and 0.54 ± 0.11 nm for AmpDNA and λ DNA, respectively.

**Note 1. Analysis of the Nature of AmpDNA.** In this experiment, we digested AmpDNA(-PPase) and AmpDNA(+PPase) with four nucleases at the optimized conditions (*i.e.* at 37 °C for 2 h with Exo I, Exo III, and Exo VII, and at 60 °C for 2 h with DSN) and resolved by 0.8% agarose gel electrophoresis (Figure S3a and S3b). The results demonstrated that the multimeric DNA products obtained from both preparations showed a smear high molecular weight band with no defined lengths. This band was significantly eliminated by treatments with Exo III and DSN, but not affected by the addition of Exo I and Exo VII. For comparison, we further tested various forms of DNA, including phage λ DNA (linear dsDNA), M13mp18 ssDNA (circular ssDNA), and synthetic DNA oligonucleotides (linear ssDNA) under the same conditions (Figure S3c-e). We observed that λ DNA and M13mp18 DNA showed similar resistance to cleavage by Exo I and Exo VII as compared with the RCA products, whereas ssDNA oligo was effectively digested by Exo I, Exo III, and Exo VII. Given that in particular DSN has a strong cleavage preference for dsDNA and little activity against ssDNA, both RCA products in solution seemingly have a mixed population of dsDNA and ssDNA, but with a large quantity of dsDNA. This double-stranded configuration can be presumably attributed to random folding of ssDNA due to intramolecular base pairing or bridging between very long, flexible DNA strands. Similar observation has been demonstrated that ssDNA grown on the surface of gold nanoparticles through RCA for 30 min appeared to merge into dsDNA-like structures in some cases.[4,5]

To confirm the results from the nuclease digestion study, we further detected both AmpDNA(-PPase) and AmpDNA(+PPase) with DNA-binding fluorescent dyes, including SYBR Green I, SYBR Green II, and SYBR Gold exhibiting specific detection sensitivity towards ssDNA and dsDNA: *i.e.* SYBR Green I represents an extremely sensitive dye for detecting dsDNA,[6] whereas SYBR Green II shows high sensitivity to detect ssDNA or RNA.[7] SYBR Gold is commonly used

as a universal dye for detecting dsDNA, ssDNA, and RNA with greatly enhanced sensitivity compared to SYBR Green I and SYBR Green II.[8] While these three dyes display binding affinity to ssDNA and dsDNA to some extent, SYBR Green I is well known to show the most pronounced enhancement of fluorescence when bound to dsDNA over ssDNA. To compare the fluorescence intensity of these dyes, serial 2-fold dilutions of DNA samples were incubated with SYBR dyes in parallel, and the fluorescence intensity was recorded. Interestingly, both AmpDNA and λ DNA showed strong fluorescence signals upon the addition of SYBR Green I, while M13mp18 ssDNA exhibited significantly low fluorescence in the presence of SYBR Green I compared to SYBR Green II. These results reveal that there are considerable amounts of dsDNA in AmpDNA regardless of the addition of PPase in the process of RCA.

**Table S2.** Properties of nucleases used in digestion of AmpDNA.

| Enzyme | Polarity | DNA substrate[a)] | | Products |
|---|---|---|---|---|
| | | ssDNA | dsDNA | |
| Exonuclease I (Exo I)[b)] | 3' → 5' | + | - | dNMP, dinucleotide |
| Exonuclease VII (Exo VII) [b)] | 3' → 5'<br>5' → 3' | + | - | Short oligos |
| Exonuclease III (Exo III) [b)] | 3' → 5' | +/- | + | ssDNA, dNMP |
| Duplex-specific nuclease (DSN) [c)] | 5' → 3' | - | + | Short oligos |

[a)]Preferred activity on DNA substrate: +, significant activity; -, no significant activity; +/-, greatly reduced activity relative to preferred substrate.
[b)]Referred to the supplier's website: https://www.neb.com/tools-and-resources/selection-charts/properties-of-exonucleases-and-endonucleases
[c)]Referred to the supplier's instructions: http://evrogen.com/protein-descriptions/UM-DSN.pdf
*Abbreviations*: dNMP, deoxyribonucleoside monophosphate; oligos, oligonucleotides.

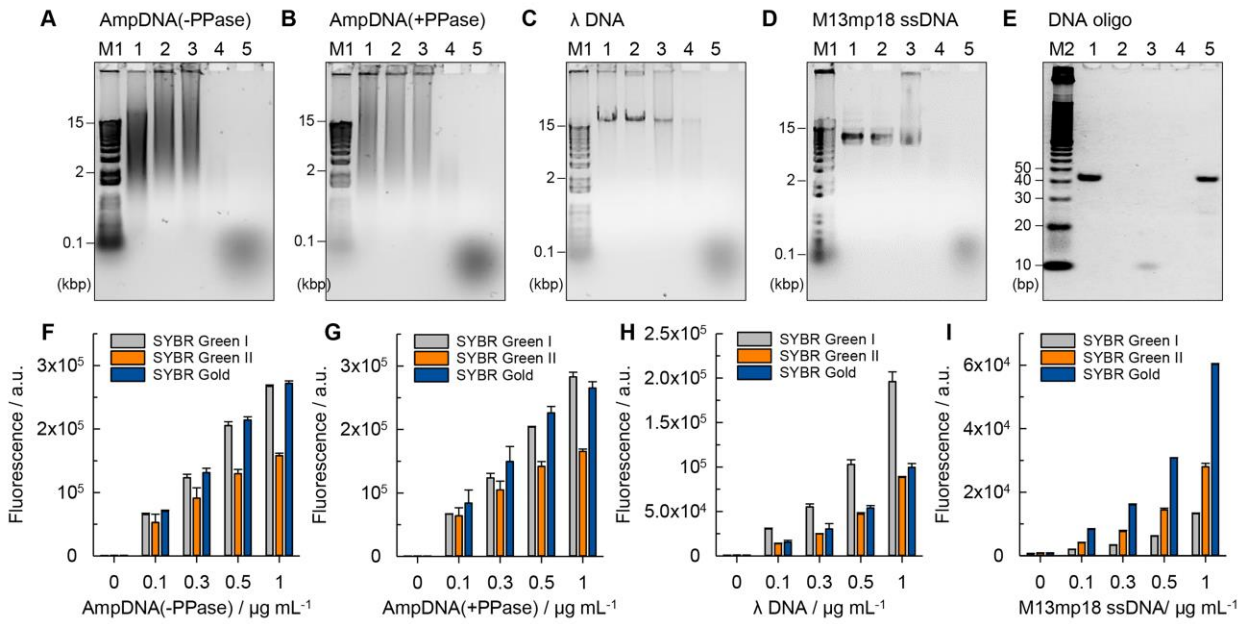


**Figure S3.** Analysis of the nature of AmpDNA. (A-E) Gel electrophoresis analysis of various DNA after digestion by ssDNA- and/or dsDNA-specific nucleases, including Exo I, Exo VII, Exo III, and DSN: (A) AmpDNA(-PPase), (B) AmpDNA(+PPase), (C) λ DNA, (D) M13mp18 ssDNA, and (E) synthetic ssDNA oligonucleotide. The resulting digested products were analyzed by (A-D) 0.8% agarose gel and (E) 10% native polyacrylamide gel electrophoresis with post-staining using SYBR Gold. Lane M1, 1 kbp DNA marker; lane M2, 10 bp DNA marker; lane 1, non-treated; lane 2, Exo I-treated; lane 3, Exo VII-treated; lane 4, Exo III-treated; lane 5, DSN-treated DNA samples. (F-I) The fluorescence intensity of serial 2-fold dilutions of DNA samples in the presence of dsDNA- and/or ssDNA-specific SYBR dyes (SYBR Green I, SYBR Green II, and SYBR Gold): (F) AmpDNA(-PPase), (G) AmpDNA(+PPase), (H) λ DNA, and (I) M13mp18 ssDNA. The fluorescence was recorded at excitation/emission of 497 nm/520 nm for SYBR Green I and SYBR Green II and 495 nm/537 nm for SYBR Gold, respectively. Data represent mean ± s.d. for three technical replicates.

**Note 2. Estimation of Average Repeating Units in AmpDNA.** From the gel image, we observed that both AmpDNA, AmpDNA(-PPase) and AmpDNA(+PPase), after EcoRV digestion were converted into two short DNA fragments around 70 and 80 nt, which are similar in size to 75 nt template DNA (Figure S4). It should be noted that the digestion products showed two DNA fragments probably due to variations in size of the AmpDNA as a result of thermal fragmentation (Figure S3a). Using ImageJ software, we compared the intensity of those two DNA bands between 70 and 80 nt to that of 50 nt loading control DNA, and calculated the average repeating units using the following equation: the average repeating unit = (($I_{\text{cleaved AmpDNA}}$ / $I_{\text{loading control}}$) × $\text{mol}_{\text{loading control}}$ × dilution factor) / $\text{mol}_{\text{DNA minicircle}}$, where $I_{\text{cleaved AmpDNA}}$ and $I_{\text{loading control}}$ are the band intensity of cleaved DNA and loading control DNA, and $\text{mol}_{\text{loading control}}$ and $\text{mol}_{\text{DNA minicircle}}$ are 100 and 30 pmol, respectively. The dilution factors were obtained by considering the dilution steps involved in the entire process: *i.e.*, for AmpDNA(-PPase), dilution from 50 μL RCA reaction volume to 100 μL elution volume (100 / 50 = 2) and from 33 ng $\mu L^{-1}$ to 25 ng $\mu L^{-1}$ of AmpDNA to hybridize with a primer (33 / 25 = 1.3), and from the volume of 25 ng $\mu L^{-1}$ AmpDNA used in digestion to the reaction volume of EcoRV digestion (20 / 0.5 = 40). This experiment was performed on three independent samples. As reported in Table S3, the average unit of AmpDNA(+PPase) was estimated to be 298.2 ± 97.8, which was slightly higher than AmpDNA(-PPase) (247.4 ± 28.5).

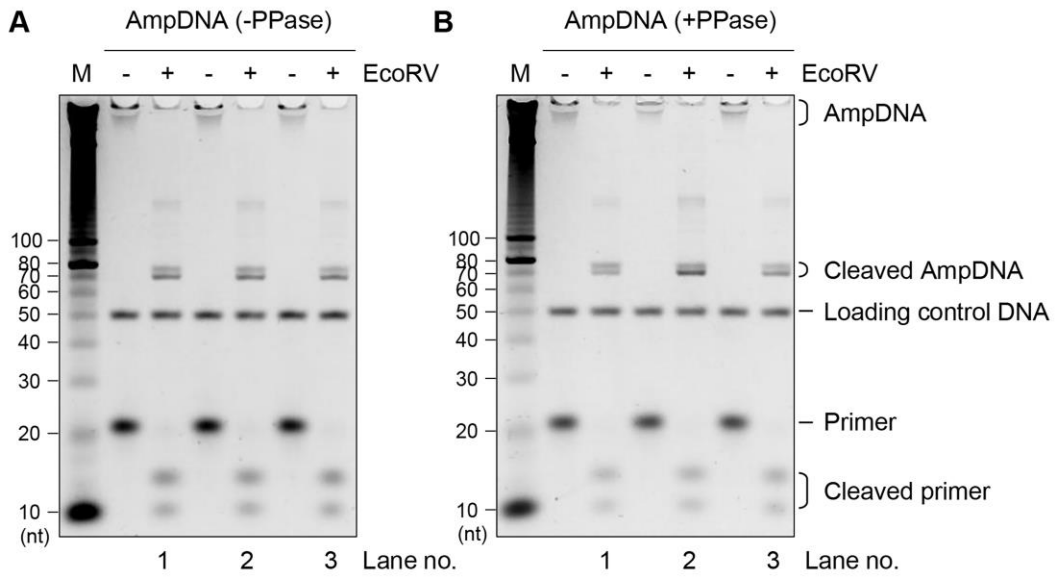


**Figure S4.** Digestion of AmpDNA by EcoRV restriction endonuclease. The AmpDNA synthesized by RCA in the (A) absence (AmpDNA(-PPase)) and (B) presence of PPase (AmpDNA(+PPase)) in triplicate were digested by EcoRV with the aid of the primer and analyzed by 10% denaturing polyacrylamide gel electrophoresis with post-staining using SYBR Gold. Non-treated AmpDNA was also run as a reference. The 50 nt DNA was co-loaded with samples as a loading control (1 pmol per lane). Lane M, 10 nt DNA marker. The band intensity of the cleaved AmpDNA around 70 to 80 nt and the loading control DNA positioned at 50 nt in lane 1-3 was used to calculate the average repeating units of AmpDNA.

**Table S3.** Estimation of average repeating units in AmpDNA.

| Sample | Lane no. | $I_{cleaved\ AmpDNA}$ | $I_{loading\ control}$ | $pmol_{loading\ control}$ | Dilution factor | $pmol_{DNA\ minicircle}$ | Repeating unit | Avg. repeating unit |
|---|---|---|---|---|---|---|---|---|
| AmpDNA (-PPase) | 1 | 6216.2 | 8255.2 | 100 | 106.9 | 30 | 268.3 | 247.4 ± 28.5 |
| | 2 | 6328.8 | 7817.8 | 100 | 96.0 | 30 | 259.1 | |
| | 3 | 5695.3 | 8650.1 | 100 | 97.9 | 30 | 214.9 | |
| AmpDNA (+PPase) | 1 | 5092.1 | 8286.5 | 100 | 99.2 | 30 | 203.2 | 298.2 ± 97.8 |
| | 2 | 9314.3 | 8127.8 | 100 | 104.3 | 30 | 398.5 | |
| | 3 | 5571.7 | 7976.8 | 100 | 125.8 | 30 | 292.8 | |

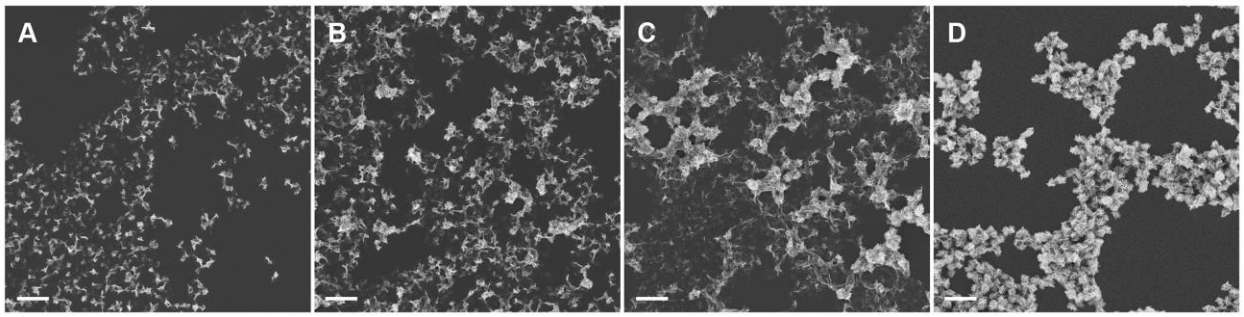


**Figure S5.** Time-dependent crystallization of $Mg_2PPi$ in the presence of AmpDNA. Representative SE-SEM images of $Mg_2PPi$/AmpDNA at various time intervals: (A) 1 h, (B) 2 h, (C) 10 h, and (D) 20 h. Scale bar, 2 μm.

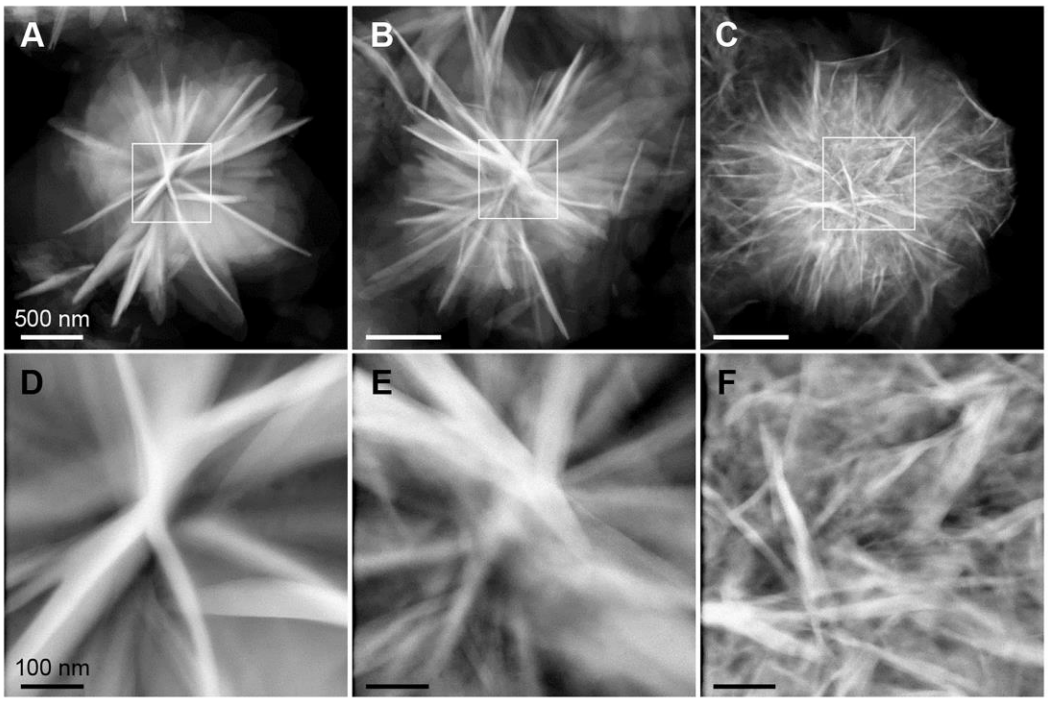


**Figure S6.** Representative HAADF-STEM images of a single $Mg_2PPi$ particle precipitated with different concentrations of PPi ions: (A, D) 0.5 mM, (B, E) 1 mM, and (C, F) 2 mM. (D-F) High-magnification images indicate HAADF-STEM images of the area marked in the solid line. Scale bars, 500 nm (A-C) and 100 nm (D-F).

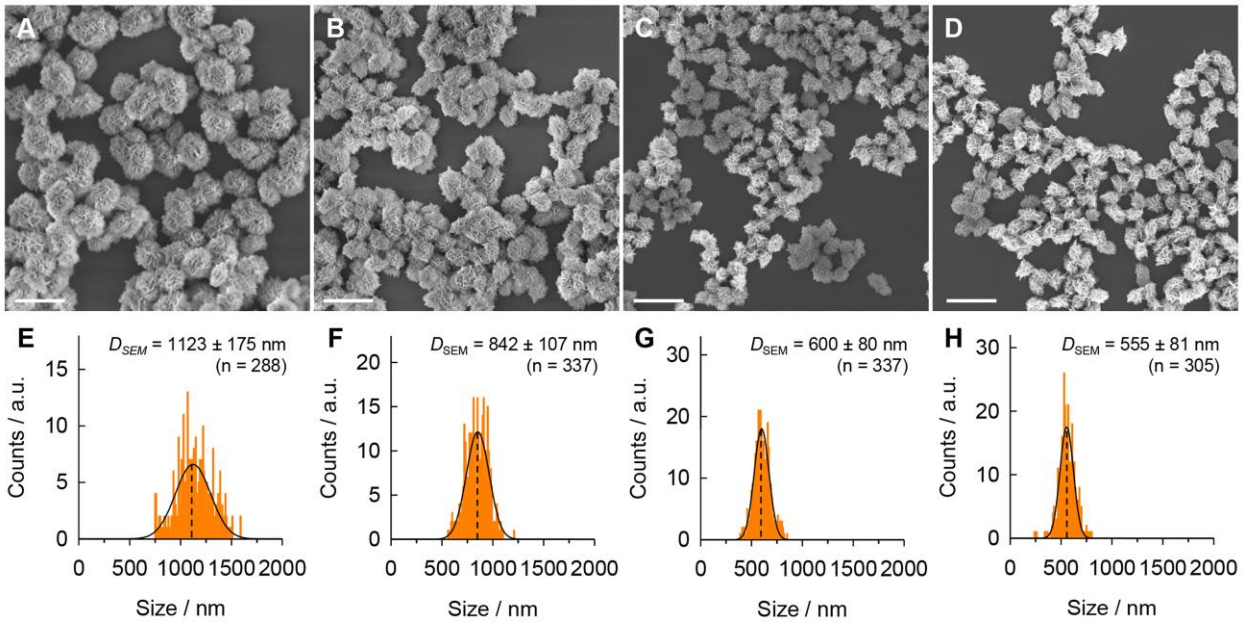


**Figure S7.** Representative (A-D) SE-SEM images and (E-H) size distribution of $Mg_2PPi$ particles grown with the addition of an increasing amount of AmpDNA: (A) 13 μg $mL^{-1}$, (B) 27 μg $mL^{-1}$, (C) 40 μg $mL^{-1}$, and (D) 67 μg $mL^{-1}$. The size distribution was determined from SEM images, fitted into the Gaussian distribution. In (E-H), the insets represent mean ± s.d. of the size analysis over about 280−340 particles per sample. Scale bar, 2 μm.

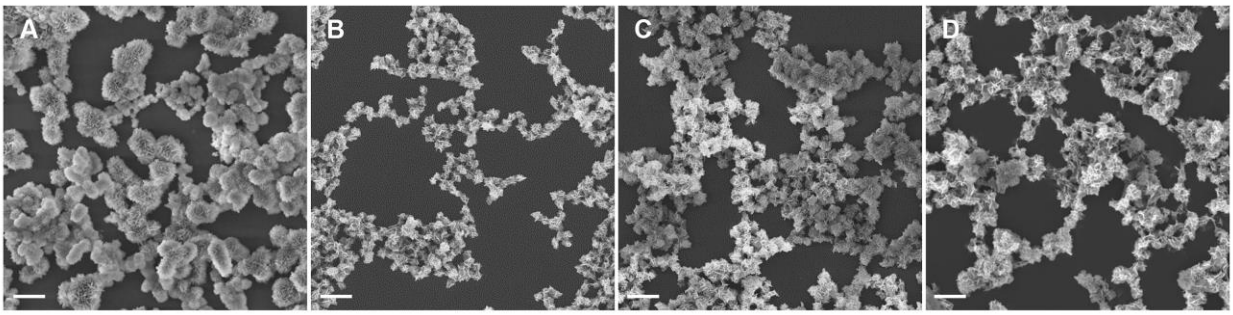


**Figure S8.** The effects of various types of DNA on formation of $Mg_2PPi$/DNA composites. Representative SE-SEM images of $Mg_2PPi$ particles prepared (A) without and (B-D) with DNA (40 μg $mL^{-1}$), including (B) AmpDNA, (C) λ DNA, and (D) M13mp18 ssDNA, respectively. Scale bar, 2 μm.

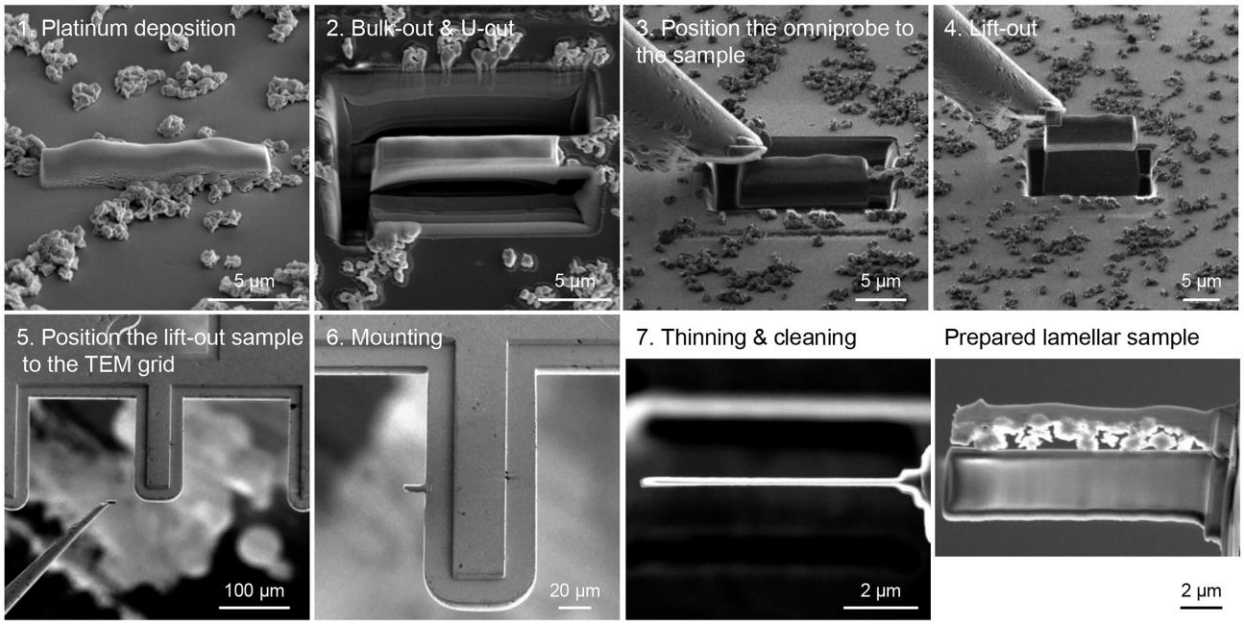


**Figure S9.** Site-specific preparation of the lamellar specimen for STEM-EELS analysis using the FIB lift-out technique.

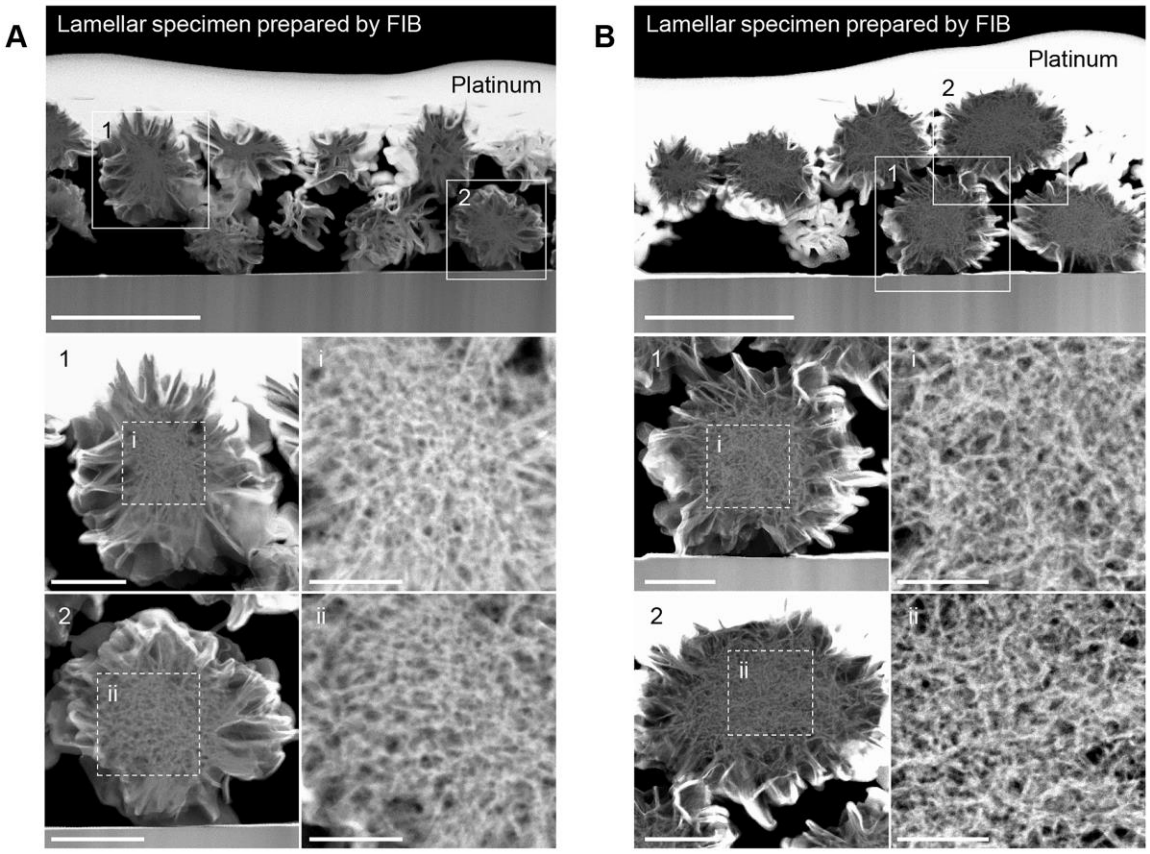


**Figure S10.** HAADF-STEM images of the lamellar specimens prepared by the FIB at different magnifications: (A) $Mg_2$PPi/AmpDNA-R and (B) DNF-R. The particles numbered 1 and 2 marked in (A) and (B) were further analysed by STEM-EELS. The obtained EELS elemental maps and spectra of the particle numbered 1 were shown in Figure 5. Scale bars, 2 μm (top), 500 nm (bottom left), 200 nm (bottom right) in (A) and (B).

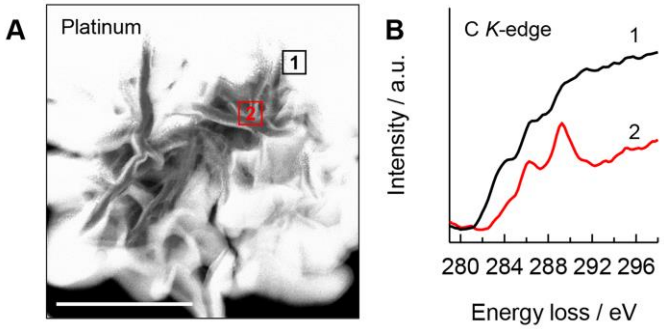


**Figure S11.** EELS reference spectrum from the platinum region. (A) HAADF-STEM image of the DNF lamellar sample and (B) EELS C *K*-edge spectra from the platinum-coated region (1) and within the sample (2), as indicated in (A). Scale bar, 500 nm.

**Note 3. SIM Imaging of Protein-Entrapped $Mg_2PPi$/AmpDNA.** We obtained additional evidence of protein encapsulation using the super-resolution structured illumination microscopy (SIM) technique, which can achieve an enhanced spatial resolution of ~100 nm in the lateral directions and simultaneous multicolor imaging with conventional fluorophores.[9] For SIM imaging, we prepared fluorescent AmpDNA by direct enzymatic incorporation of Cy3-modified deoxynucleotides (dNTPs) during RCA, followed by subsequent isolation with ethanol precipitation. We also coupled RNase A with N-hydroxysuccinimide fluorescein before precipitation with $Mg_2PPi$. For comparison, we synthesized fluorescent DNF and DNF-R by performing RCA with Cy3-labeled dNTPs and a fluorescein-labeled enzyme. We then collected 3D SIM z-stacks of each particle, in which DNA or enzymes could be identified as fluorescent signals inside the particles (Figure S12). Consistent with DNF, the cross-sections of $Mg_2PPi$/AmpDNA composites were homogeneously fluorescent. More interestingly, the enzyme encapsulation in $Mg_2PPi$ showed distinct localization compared to DNA-associated particles, where RNase A was predominantly located on the periphery of the surface of $Mg_2PPi$ without DNA, while it was evenly distributed in the entire region of $Mg_2PPi$/AmpDNA or DNF. This result can be attributed to the presence of DNA molecules that impede the rapid growth of crystals and electrostatically interact with positively charged RNase A. This leads to trapping of proteins into the hydrated polymer-like DNA network throughout particles, not only at their surfaces.

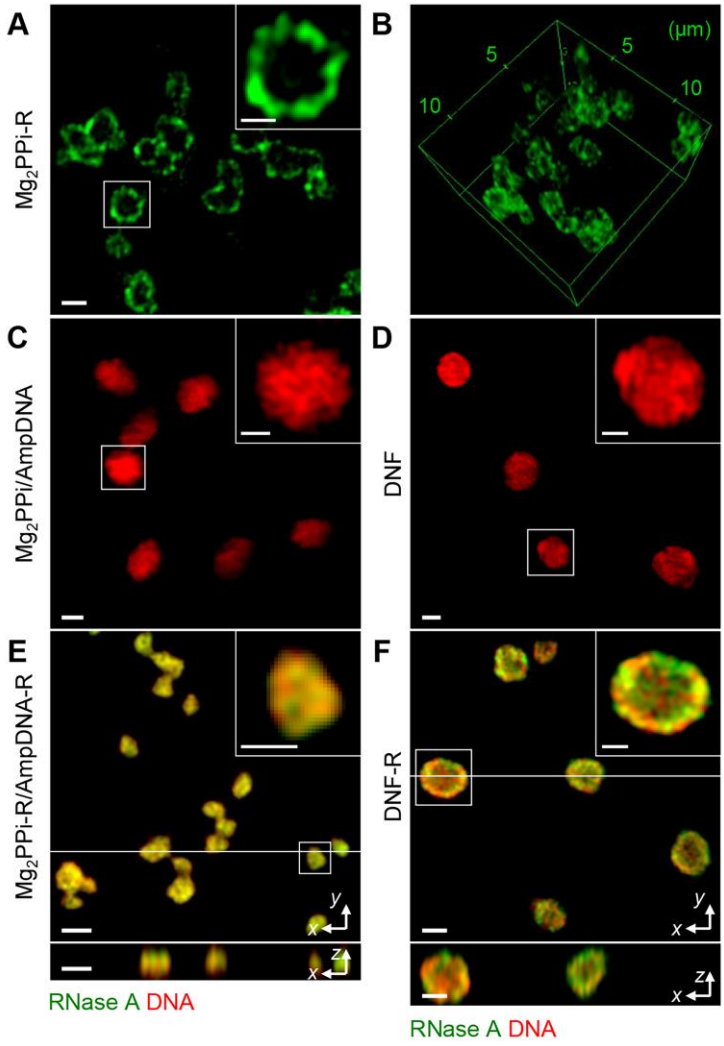


**Figure S12.** 3D SIM imaging of DNA- and/or enzyme-incorporated $Mg_2PPi$ composites. (A) 2D cross-sectional and (B) 3D reconstructed images of $Mg_2PPi$-R, cross sections of (C) $Mg_2PPi$-R/AmpDNA, (D) DNF, (E) $Mg_2PPi$/AmpDNA-R, and (F) DNF-R. In (E) and (F), orthogonal cross sections were also shown. RNase A and DNA were labeled with fluorescein (green) and Cy3 (red), respectively. Insets indicate higher magnification views of the region marked by the white box in the main image. Scale bars, 1 μm (main panels) and 0.5 μm (inset panels).

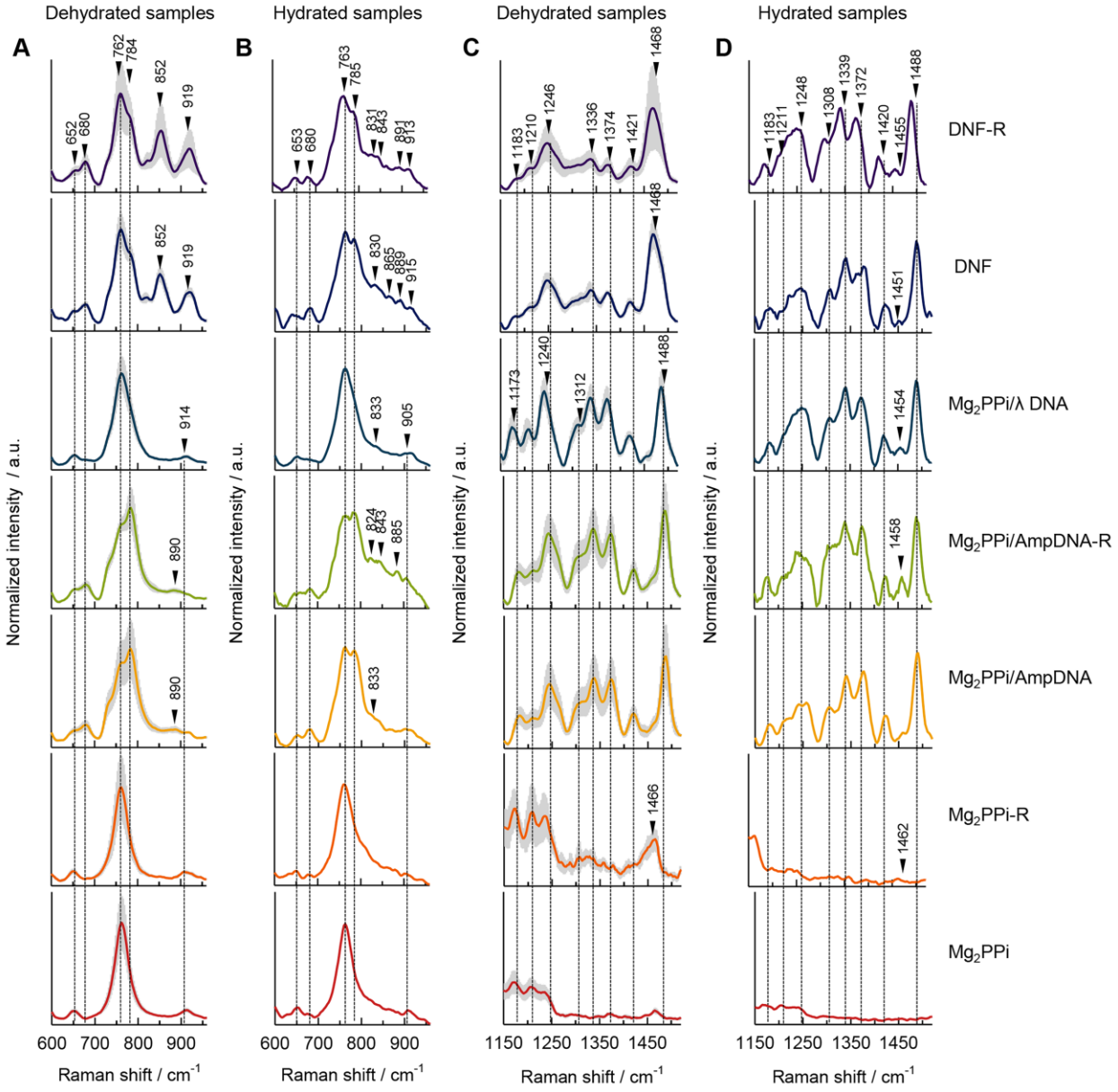


**Figure S13.** Comparison of Raman spectra over the range of (A, B) 600−920 $cm^{-1}$ and (C, D) 1150−1520 $cm^{-1}$ for each $Mg_2PPi$ composite prepared by a co-precipitation method or a one-pot RCA process. For Raman measurements, (A, C) the solid films prepared by evaporation of aqueous sample solution and (B, D) droplets of aqueous solution samples on a calcium fluoride substrate were used. The spectra in (A) and (C) show the average spectra ± s.d. of five different points randomly selected in the sample. The spectra in (B) and (D) show representative spectra of one point in the sample.

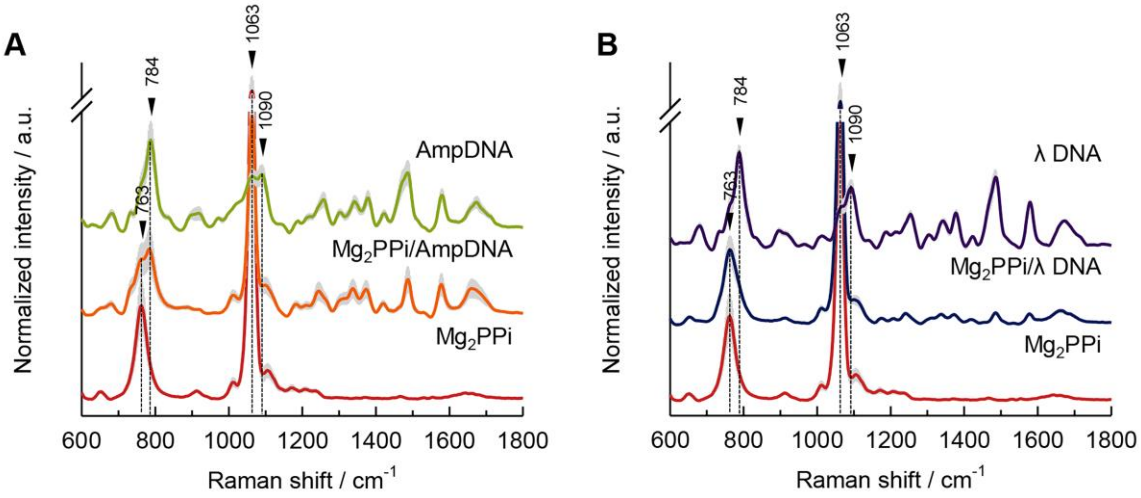


**Figure S14.** Raman spectra of (A) $Mg_2PPi$, $Mg_2PPi$/AmpDNA, and AmpDNA, and (B) $Mg_2PPi$, $Mg_2PPi$/λ DNA, and λ DNA, prepared by evaporation of aqueous sample solution. The spectra show the average spectra ± s.d. of five different points randomly selected in the sample .

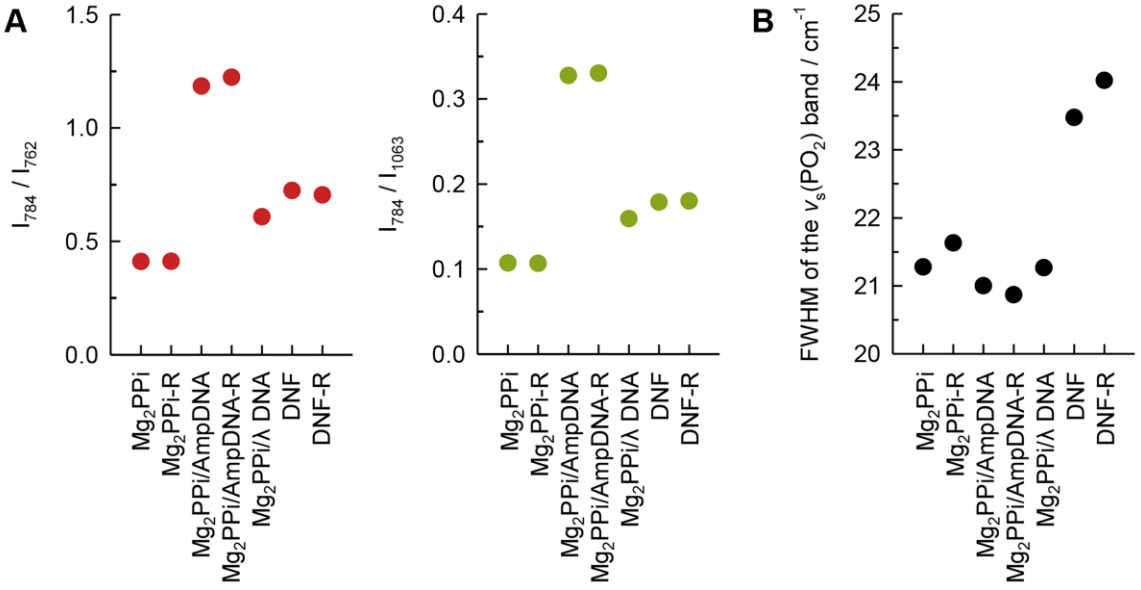


**Figure S15.** (A) Intensity ratio of the signals for the $\nu_s$(OPO) band at 784 $cm^{-1}$, the $\nu_s$(POP) at 762 $cm^{-1}$, and the $\nu_s(PO_2)$ band at 1063 $cm^{-1}$, and (B) FWHM of the $\nu_s(PO_2)$ band centered at 1063 $cm^{-1}$ for different $Mg_2PPi$ composites.

**Table S4.** Tentative Raman band assignment of various $Mg_2PPi$ composites measured in dehydrated forms.

| $Mg_2PPi$ | $Mg_2PPi$-R | $Mg_2PPi$/AmpDNA | $Mg_2PPi$/AmpDNA-R | $Mg_2PPi$/λ DNA | DNF | DNF-R | AmpDNA | λ DNA | Assignment[a)] |
|---|---|---|---|---|---|---|---|---|---|
| | | 680 | 680 | 681 | 678 | 678 | 682 | 680 | dG |
| 763 | 763 | 763 | 762 | 763 | 763 | 762 | | | $\nu_s$(POP) |
| | | 784 | 784 | | 783 | 783 | 786 | 788 | $\nu_s$(OPO) |
| | | | | | | | 833 | 833 | $\nu_s$(OPO) |
| | | | | | 853 | 855 | | | Tyr |
| | | 890 | 887 | 887 | | | | | Deoxy |
| 912 | 910 | 918 | 918 | 912 | | | 914 | 908 | $\nu_{as}$(POP) |
| | | | | | 920 | 920 | | | Glu |
| 1013 | 1011 | 1013 | 1011 | 1013 | 1011 | 1011 | 1020 | 1017 | $\nu_s(PO_3)$ |
| 1063 | 1063 | 1063 | 1063 | 1063 | 1062 | 1062 | 1063 | 1068 | $\nu_s(PO_2)$ |
| 1105 | 1103 | 1100 | 1100 | 1102 | 1100 | 1100 | 1090 | 1092 | $\nu_s(PO_2)$ |
| 1172 | 1172 | | | | | | | | $\nu_{as}(PO_3)$ |
| | | | | | | | 1141 | 1137 | Deoxy |
| | | 1182 | 1182 | 1176 | 1182 | 1188 | 1186 | 1188 | dT |
| 1206 | 1208 | 1211 | 1212 | 1206 | 1212 | 1212 | 1218 | 1218 | $\nu_{as}(PO_2)$ |
| 1237 | 1236 | | | | | | | | $\nu_{as}(PO_2)$ |
| | | 1245 | 1243 | 1241 | 1247 | 1247 | 1255 | 1255 | dC, dT |
| | | 1308 | 1310 | 1312 | 1310 | 1314 | 1302 | 1304 | dA, dC |
| | | 1338 | 1336 | 1338 | 1338 | 1336 | 1344 | 1342 | dA, dG |
| | | 1373 | 1373 | 1373 | 1373 | 1373 | 1377 | 1377 | dT |
| | | 1420 | 1420 | 1420 | 1420 | 1423 | 1423 | 1423 | 2' $CH_2$ |
| | 1464 | | | | 1470 | 1468 | | | Ala |
| | | 1488 | 1488 | 1486 | | | 1486 | 1486 | dA, dG |
| | | 1578 | 1578 | 1578 | 1578 | 1578 | 1580 | 1580 | dA, dG |
| | | 1661 | 1665 | 1663 | 1663 | 1669 | 1673 | 1671 | dT |

[a)]Abbreviations: $\nu_s$, symmetric stretching; $\nu_{as}$, asymmetric stretching; δ, bending; POP, POP bridge; OPO, phosphodiester backbone; $PO_2$ or $PO_3$, anionic phosphate group; Deoxy, Deoxyribose; dA, deoxyadenine; dC, deoxycytosine; dG, deoxyguanine; dT, deoxythymine; Tyr, Tyrosine; Glu, Glutamic acid; Ala, Alanine.

**Table S5.** Tentative Raman assignment of various $Mg_2PPi$ composites measured in hydrated forms.

| $Mg_2PPi$ | $Mg_2PPi$-R | $Mg_2PPi$/ AmpDNA | $Mg_2PPi$/ AmpDNA-R | $Mg_2PPi$/ λ DNA | DNF | DNF-R | Assignment[a)] |
|---|---|---|---|---|---|---|---|
| | | 680 | 684 | 673 | 681 | 681 | dG |
| 763 | 763 | 763 | 767 | 763 | 764 | 764 | $v_s$(POP) |
| | | 784 | 784 | | 782 | 785 | $v_s$(OPO) |
| | | 832 | 831 | 834 | 831 | 831 | $v_s$(OPO) |
| | | | 842 | | 862 | 842 | Tyr |
| | | 867 | 887 | | 891 | 891 | Deoxy |
| 908 | 905 | 902 | 906 | 909 | 914 | 914 | $v_{as}$(POP) |
| | | | 969 | | | | Glu |
| 1013 | 995 | 1011 | 1007 | 1012 | 1012 | 1010 | $v_s(PO_3)$ |
| 1062 | 1062 | 1062 | 1062 | 1062 | 1062 | 1062 | $v_s(PO_2)$ |
| 1109 | 1111 | 1093 | 1094 | 1097 | 1092 | 1095 | $v_s(PO_2)$ |
| 1168 | 1160 | | | | | | $v_{as}(PO_3)$ |
| | | 1180 | 1176 | 1175 | 1180 | 1183 | dT |
| 1206 | 1198 | 1218 | 1212 | 1209 | 1209 | 1211 | $v_{as}(PO_2)$ |
| 1237 | 1237 | | | | | | $v_{as}(PO_2)$ |
| | | 1241 | 1241 | 1240 | 1249 | 1248 | dC, dT |
| | | 1306 | 1306 | 1307 | 1307 | 1307 | dA, dC |
| | | 1340 | 1338 | 1338 | 1341 | 1341 | dA, dG |
| | | 1375 | 1375 | 1377 | 1379 | 1372 | dT |
| | | 1424 | 1422 | 1421 | 1423 | 1421 | 2' $CH_2$ |
| | | | 1458 | | 1454 | 1454 | dT |
| | | 1489 | 1489 | 1488 | 1488 | 1488 | dA, dG |
| | | 1580 | 1586 | 1584 | 1581 | 1584 | dA, dG |
| 1643 | 1643 | 1653 | 1653 | 1650 | 1650 | 1648 | $\delta H_2O$ |
| | | 1660 | 1663 | 1664 | 1664 | 1664 | dT |

[a)]Abbreviations: $v_s$, symmetric stretching; $v_{as}$, asymmetric stretching; δ, bending; POP, POP bridge; OPO, phosphodiester backbone; $PO_2$ or $PO_3$, anionic phosphate group; Deoxy, Deoxyribose; dA, deoxyadenine; dC, deoxycytosine; dG, deoxyguanine; dT, deoxythymine; Tyr, Tyrosine; Glu, Glutamic acid; Ala, Alanine.

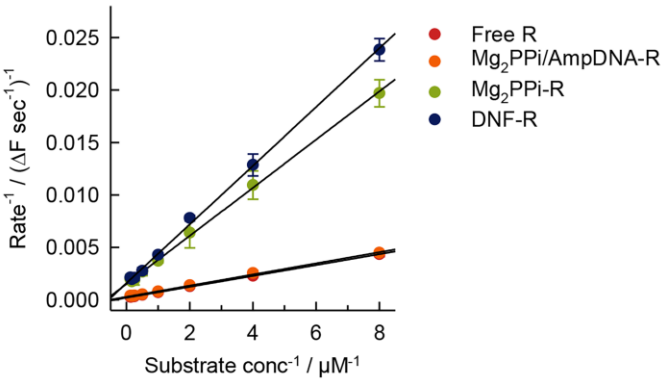


**Figure S16.** Lineweaver-Burk plot of free RNase A (R), $Mg_2PPi$/AmpDNA-R, $Mg_2PPi$-R, and DNF-R. The concentration of RNase A in each sample was 0.5 ng $mL^{-1}$. Results represent mean ± s.d. for four independent experiments.

**Table S6.** Enzyme kinetics showing the Michaelis-Menten constant ($K_m$) and maximum velocity ($V_{max}$) of free enzyme and the encapsulated enzyme in $Mg_2PPi$/AmpDNA, $Mg_2PPi$, and DNF. Data represent mean ± s.d. for four independent experiments.

| Sample | $K_m$ / μM | $V_{max}$ / ΔF $sec^{-1}$ |
|---|---|---|
| Free RNase A | 2.5 ± 0.2 | 4913.2 ± 187.1 |
| $Mg_2PPi$/AmpDNA-R | 1.8 ± 0.03 | 3460.4 ± 119.3 |
| $Mg_2PPi$-R | 1.5 ± 0.1 | 668.4 ± 83.9 |
| DNF-R | 1.8 ± 0.1 | 628.7 ± 49.5 |

## References

(1) Hermanowicz, P.; Sarna, M.; Burda, K.; Gabryś, H. AtomicJ: An Open Source Software for Analysis of Force Curves. *Rev. Sci. Instrum.* **2014**, *85*, 063703.

(2) Liu, M.; Hui, C. Y.; Zhang, Q.; Gu, J.; Kannan, B.; Jahanshahi-Anbuhi, S.; Filipe, C. D. M.; Brennan, J. D.; Li, Y. Target-Induced and Equipment-Free DNA Amplification with a Simple Paper Device. *Angew. Chem. Int. Ed.* **2016**, *55*, 2709-2713.

(3) Liu, M.; Zhang, Q.; Kannan, B.; Botton, G. A.; Yang, J.; Soleymani, L.; Brennan, J. D.; Li, Y. Self-Assembled Functional DNA Superstructures as High-Density and Versatile Recognition Elements for Printed Paper Sensors. *Angew. Chem. Int. Ed.* **2018**, *57*, 12440-12443.

(4) Zhao, W.; Gao, Y.; Kandadai, S. A.; Brook, M. A.; Li, Y. DNA Polymerization on Gold Nanoparticles Through Rolling Circle Amplification: Towards Novel Scaffolds for Three-Dimensional Periodic Nanoassemblies. *Angew. Chem. Int. Ed.* **2006**, *45*, 2409-2413.

(5) Yan, J.; Hu, C.; Wang, P.; Zhao, B.; Ouyang, X.; Zhou, J.; Liu, R.; He, D.; Fan, C.; Song, S. Growth and Origami Folding of DNA on Nanoparticles for High-Efficiency Molecular Transport in Cellular Imaging and Drug Delivery. *Angew. Chem. Int. Ed.* **2015**, *54*, 2431-2435.

(6) Zipper, H.; Brunner, H.; Bernhagen, J.; Vitzthum, F. Investigations on DNA Intercalation and Surface Binding by SYBR Green I, Its Structure Determination and Methodological Implications. *Nucleic Acids Res.* **2004**, *32*, e103.

(7) Lee, L. G.; Chen, C.-H.; Chiu, L. A. Thiazole Orange: A New Dye for Reticulocyte Analysis. *Cytometry* **1986**, *7*, 508-517.

(8) Tuma, R. S.; Beaudet, M. P.; Jin, X.; Jones, L. J.; Cheung, C.-Y.; Yue, S.; Singer, V. L. Characterization of SYBR Gold Nucleic Acid Gel Stain: A Dye Optimized for Use with 300-nm Ultraviolet Transilluminators. *Anal. Biochem.* **1999**, *268*, 278-288.

(9) Huang, B.; Babcock, H.; Zhuang, X. Breaking the Diffraction Barrier: Super-Resolution Imaging of Cells. *Cell* **2010**, *143*, 1047-1058.